Modelling of the influence of dihedral angle, volume fractions, particle size and coordination on the driving forces for sintering of dual phase systems

Francis Delannay

Modelling of the influence of dihedral angle, volume fractions, particle size and coordination on the driving forces for sintering of dual phase systems

Journal:	*Philosophical Magazine & Philosophical Magazine Letters*
Manuscript ID:	TPHM-05-Aug-0367.R1
Journal Selection:	Philosophical Magazine
Date Submitted by the Author:	20-Aug-2005
Complete List of Authors:	Delannay, Francis; Université catholique de Louvain, matériaux et des procédés (MAPR)
Keywords:	wetting, sintering, interfacial thermodynamics
Keywords (user supplied):	

Submitted to Philosophical Magazine

Modelling of the influence of dihedral angle, volume fractions, particle size and coordination on the driving forces for sintering of dual phase systems

Francis DELANNAY*

Université catholique de Louvain, Département des Sciences des matériaux et des procédés, IMAP, Place Sainte Barbe 2, B-1348 Louvain-la-Neuve, Belgium

Abstract

The equilibrium shape of solid particles in an aggregate immersed in a liquid or in a gas results from the minimisation of interface energy. A model is developed for expressing the dependence of the solid/solid and solid/second phase interface areas on the system parameters : phase volume fractions, dihedral angle, particle size and coordination. The model aims at allowing quantitative assessment of the role of these parameters on the driving force for sintering. The representative volume element is a cone of which the apex angle accounts for the average particle coordination. In order to comply with the uniformity of interface curvature, the solid/second phase interfaces are described using the mathematics of the Delaunay surfaces. The results are compared with the solutions obtained by approximating the interface shape by the revolution of an arc of circle around the cone axis. This approximation reveals not to involve significant loss of precision.

* E-mail address : Delannay@imap.ucl.ac.be. Tel : 0032 10 47 24 26 ; fax : 0032 10 47 40 28.

1 Introduction

The system analysed in this paper is sketched in Fig. 1a. It consists of an aggregate of solid particles immersed in a fluid phase, which may be either a gas or a liquid, that completely fills the pores between the particles. The equilibrium shape of the particles results from the minimisation of interface energy. Proper understanding of the thermodynamics of such a system is a condition for the modelling of the kinetics of microstructural evolution during sintering in the presence of a gaseous or liquid phase [1 – 6]. A point of particular interest in this context is the phenomenon of shape accommodation during liquid phase sintering, which governs the redistribution of the liquid during sintering of materials with functionally designed composition gradients [7 – 12].

(Figure 1)

We will denote V_s the volume of the solid phase, V_{fl} the volume of the fluid phase (meaning either a liquid or a gas) filling the pores, and V_{excess} the volume of fluid surrounding the aggregate (Fig.1). The volume fraction, u, of fluid phase inside the aggregate is thus

$$u = \frac{V_{fl}}{V_{fl} + V_s} \tag{1}$$

and the average volume of the solid particles, V_p, is

$$V_p = \frac{V_s}{n_p} \tag{2}$$

where n_p is the number of particles in the aggregate. $V_p^{1/3}$ is a measure of the average particle size. As illustrated in Fig.2, it is convenient to consider that each particle in the aggregate is enclosed into a Voronoï cell, the faces of which are the planes bisecting the vectors connecting of the centre of gravity of the particle to the centres of gravity of all surrounding

particles [e.g. 13] (in Fig. 2, the solid/solid interfaces are represented as located at the position of the cell faces). As the ensemble of Voronoï cells perfectly fills the space, the average cell volume V_{VC} is

$$V_{VC} = \frac{V_{fl} + V_s}{n_p} = \frac{V_p}{1-u}. \quad (3)$$

The mode of packing of the particles is characterised by the shape of the Voronoï cell. The coordination number, n_c, of each particle may be defined as the number of faces of the Voronoï cell. According to the works of Scott [14] and Mason [15], the average coordination number in a random packing would be close to 7.3 [13].

(Figure 2)

The excess free energies per unit area of solid/fluid and solid/solid interfaces will be denoted γ_{sfl} and γ_{ss}, respectively. As represented in Fig. 1b, if $\gamma_{sfl} \geq \gamma_{ss}/2$,

$$\gamma_{ss} = 2\gamma_{sfl} \cos\left(\frac{\psi}{2}\right) \quad (4)$$

where ψ is the dihedral angle. If $\gamma_{sfl} \leq \gamma_{ss}/2$, $\psi = 0$, the boundary between two solid particles is wetted by a thin liquid or gaseous film [16 - 19] and the excess free energy per unit area associated with this boundary is then equal to $2\gamma_{sfl}$. In this case, the volume of fluid associated with this film separating the particles will be supposed to be negligible in comparison to the total volume of fluid filling the pores. Although the analysis could be extended to more complex cases [12], the present work deals only with the case when γ_{sfl} and γ_{ss} are isotropic, i.e. independent of the interface orientation with respect to the crystal lattice. Hence, when the fluid volume fraction exceeds a critical value, the equilibrium shapes of the particles become simple spheres.

In this work, the solid and fluid phases are supposed to be in overall chemical equilibrium, i.e. the chemical potentials of their constituents are supposed to be identical in the two phases. In addition, both phases are modelled as being incompressible. Obviously, this approximation is invalid when the fluid is a gas. Nevertheless, we believe that, although not accounting for the compressibility of the gas phase, the model allows gaining useful insight even into the process of sintering in solid-gas systems. The evolution of the system is thus considered to be driven by the mere decrease of the excess free energy F associated with solid/fluid and solid/solid interfaces, which writes

$$F = \gamma_{\mathrm{sfl}} A_{\mathrm{sfl}} + \gamma_{\mathrm{ss}} A_{\mathrm{ss}} = \gamma_{\mathrm{sfl}} \left[A_{\mathrm{sfl}} + 2\cos\left(\frac{\psi}{2}\right) A_{\mathrm{ss}} \right] \tag{5}$$

where A_{sfl} and A_{ss} are the total solid/fluid and solid/solid interface areas. As γ_{sfl} acts as a simple scaling parameter, the only significant material parameter is the dihedral angle ψ. A decrease of F can be brought about by a change of the particle sizes $V_{\mathrm{p}}^{1/3}$ and/or by a change of particle shapes. A change of shape without change of size may result from a change of the coordination n_{c} and/or from the addition or subtraction of some fluid volume dV_{fl} in the pores. The driving forces for the evolution of the system can thus be expressed as partial derivatives of F with respect to $V_{\mathrm{p}}^{1/3}$, n_{c}, and V_{fl} (or u). The purpose of the present work is to make possible the computation of these driving forces by modelling the dependence of A_{sfl} and A_{ss} on $V_{\mathrm{p}}^{1/3}$, n_{c}, u and ψ at thermodynamic equilibrium.

2 Model

As represented in Fig.2, owing to the wetting mechanisms, the liquid phase is situated at the cell apexes and, if u is high enough, along the length of the cell edges [20, 21]. When u

increases, the solid/solid interface contracts on the central part of the face of the cell until it becomes restricted to a point. Beyond this stage, the particles assume the shape of spheres. The Voronoï cell thus consists of an assembly of n_c pyramidal prisms of which the apex is the particle centre of gravity and the basis is one of the cell faces, the liquid phase being segregated at the corners and along the edges of the pyramid basis. As illustrated in Fig.3, the model developed in the present paper consists in substituting these pyramids by cones of revolution of which the axis is the vector connecting the centres of gravity of the particles in contact. The average Voronoï cell is thus modelled as equivalent to n_c identical cones. The volume of this representative cone is

$$V_{\text{cone}} = \frac{V_{\text{VC}}}{n_c} = \frac{V_{\text{p}}}{n_c(1-u)}. \qquad (6)$$

The height of the cone is the average distance, H, between the particles centre of gravity and the Voronoï cell faces. By symmetry, the solid/liquid interface meets the lateral surface of the cone at 90°.

(Figure 3)

A limitation of the model is that the fluid is considered to keep the shape of a circular channel circumscribing the solid/solid interface boundary. It is well known that, due to the Raleigh instability, cylindrical channels can spontaneously fragment into a series of isolated spheres when the ratio of the length to the radius of the channel becomes larger than a critical value. When modelling sintering in solid-gas systems, this phenomenon is commonly considered to cause the transition between the second stage of sintering, during which the pores are assumed to form a fully interconnected network, and the third stage of sintering, during which the pores are assumed to be isolated from one another. Hence, the validity of

the present model will be questionable at low fluid volume fraction when extensive fragmentation of the fluid channels can have developed.

The model is fully characterised by the average particle volume, V_p, and the average particle coordination, n_c, in the aggregate. Indeed, we can assume that, at the beginning of the sintering process, no solid/solid interface is yet created and the particles are then simple spheres in contact with one another. The sum of the surface areas developed by the spherical solid/fluid interfaces in the n_c cones must then be equal to the surface area of a sphere. This writes

$$n_c\, 2\pi H^2 (1-\cos\beta) = 4\pi H^2 \tag{7}$$

where β is the half angle at the cone apex (Fig.3). Hence, β derives from the average coordination number n_c of the particles :

$$\beta = \arccos\left(1-\frac{2}{n_c}\right). \tag{8}$$

Notice that the model does not require n_c to be an integer. When the particles are simple spheres in contact with one another, u reaches a critical value u_m which expresses as

$$u_m = \frac{\frac{\pi}{3}H^3\tan^2\beta - \frac{4\pi H^3}{3n_c}}{\frac{\pi}{3}H^3\tan^2\beta} = 1-\frac{4}{n_c\tan^2\beta} = \frac{3n_c-4}{n_c(n_c-1)}. \tag{9}$$

It can easily be verified that the u_m values expressed by (9) agree fairly well with the u_m values for regular packings of spheres : primitive cubic (n_c = 6, u_m = 0.4764), body centred cubic (n_c = 8, u_m = 0.3198), and closed-packed (n_c = 12, u_m = 0.2424) [12]. When u = 0, the sum of the volumes of the n_c cones must be equal to V_p, which yields

$$V_p = V_{VC} = n_c\frac{\pi}{3}H^3\tan^2\beta = \frac{4\pi}{3}\frac{n_c(n_c-1)}{(n_c-2)^2}H^3. \tag{10}$$

As represented in Fig. 4, let us consider an orthogonal system of axes of which the origin is at the centre of the cone basis, with coordinate axis X parallel to the basis, and Y pointing to the cone apex. Plane (X, Y) intersects the solid/fluid interface along a curve $Y(X)$, which depends on the parameters u, β, and $\psi/2$ (for the needs of what follows, the surface occupied by the fluid is, in Fig.4, divided in two parts S_a and S_b). It is convenient to convert X and $Y(X)$ into non-dimensional variables :

$$x = \frac{X}{H} \; ; \tag{11}$$

$$y(x) = \frac{Y(X)}{H} \, . \tag{12}$$

The ranges for x and $y(x)$ are thus $0 \le x \le \tan\beta$ and $0 \le y(x) \le 1$. We will denote $y'(x)$ ($= \tan\theta$: see Fig.4) and $y''(x)$ the first and second derivatives of $y(x)$. The boundary points of the curve at coordinates ($x_{\min}$, 0) and ($x_{\max}$, $y_{\max}$) are thus such that

$$x_{\max} = (1 - y_{\max}) \tan\beta \, , \tag{13}$$

$$y'_{y=y_{\max}} = \tan\beta \, , \tag{14}$$

and $$y'_{y=0} = \tan\frac{\psi}{2} \, . \tag{15}$$

The two principal radii of curvature of the solid/fluid interface are respectively parallel and perpendicular to plane (X, Y) and will be denoted $R_{\text{in plane}}$ and $R_{\text{out of plane}}$. If s is the curvilinear coordinate along $y(x)$, it is easy to derive

$$\frac{H}{R_{\text{in plane}}} = \frac{d\theta}{ds} = \frac{y''}{(1 + y'^2)^{3/2}} \, . \tag{16}$$

(see for example Eq. 3 in [22]). $R_{\text{in plane}}$ can thus be either positive (i.e. pointing towards the cone axis) or negative. On another hand, the solid/fluid interface being generated by the

revolution of the y(x) curve around the cone axis, reference to Fig.4 indicates that $R_{\text{out of plane}}$ is related to $y'(x)$ as

$$\frac{R_{\text{out of plane}}}{H} = \frac{x}{\sin\theta} = x\sqrt{\frac{1+y'^2}{y'^2}}. \tag{17}$$

$R_{\text{out of plane}}$ is thus always positive.

(Figure 4)

u, A_{sfl} and A_{ss} are univocally determined by the curve $Y(X)$. Firstly, the volume of fluid in the representative cone is the volume created by the revolution of the surface $S_a + S_b$ around the cone axis (Fig.4). The revolution of S_a and S_b creates two volumes V_a and V_b, respectively, which express as

$$V_a = 2\pi H^3 \int_{x_{\min}}^{x_{\max}} xy\,dx \tag{18}$$

and

$$V_b = 2\pi H^3 \left(x_{\max} + \frac{\tan\beta - x_{\max}}{3} \right) \frac{(\tan\beta - x_{\max})^2}{2\tan\beta}. \tag{19}$$

The fluid volume fraction is thus

$$u = \frac{V_l}{nV_{VC}} = \frac{6}{\tan^2\beta}\left[\int_{x_{\min}}^{x_{\max}} xy\,dx + \left(x_{\max} + \frac{\tan\beta - x_{\max}}{3} \right) \frac{(\tan\beta - x_{\max})^2}{2\tan\beta} \right] \tag{20}$$

where use has been made of relation (10). Secondly, the solid/fluid interface area is created by a revolution of the curve $Y(X)$ around the cone axis. Denoting Hds an increment of length along the curve $Y(X)$, A_{sfl} writes

$$A_{\text{sfl}} = n\,n_c H^2 2\pi \int_{(x_{\min}, y_{\min})}^{(x_{\max}, y_{\max})} x\,ds \tag{21}$$

or, alternatively,

$$A_{\mathrm{sfl}} = n\, n_{\mathrm{c}} H^2 2\pi \int_{x_{\min}}^{x_{\max}} x\sqrt{1+y'^2}\,dx\,. \tag{22}$$

Finally, as $Hx_{\min}$ is the radius of the circle circumscribing the solid/solid interface, the total solid/solid interface area is simply

$$A_{\mathrm{ss}} = \frac{n}{2} n_{\mathrm{c}} H^2 \pi\, x_{\min}{}^2\,. \tag{23}$$

Relations (20), (22), and (23) provide all the ingredients needed for expressing, according to (5), the variation of the free energy F of the system as a function of the parameters $V_{\mathrm{p}}^{1/3}$, n_{c}, u, and ψ.

3 Results and discussion

3.1 Exact solution

At thermodynamic equilibrium, for any value of u, $y(x)$ is the curve that both complies with the boundary conditions (13 – 15) and brings about a minimum of the interface energy (5). This amounts to the solution of a variational problem [21, 23]. Alternatively, the curve $y(x)$ can be derived on the basis of the fact that, when the interface area has reached its minimum, the curvature of the solid/fluid interface is constant everywhere :

$$\frac{1}{R_{\text{in plane}}} + \frac{1}{R_{\text{out of plane}}} = \frac{1}{R_{\mathrm{av}}} = \frac{1}{r_{\mathrm{av}} H} \tag{24}$$

where r_{av} is the constant average curvature which depends on the parameters u, β, and $\psi/2$. Hence, using (16) and (17), $y(x)$ is a solution of the differential equation

$$y'' + y'\left(1+y'^2\right)\frac{1}{x} - \frac{1}{r_{\mathrm{av}}}\left(1+y'^2\right)^{3/2} = 0\,. \tag{25}$$

in which the value of r_{av} derives from the three boundary conditions (13) to (15). A convenient procedure for solving equation (25) numerically is to make use of the two conditions (13) and (14) and to adjust iteratively the value of the parameter r_{av} for finding the solution that complies with the third condition (15).

Instead of computing $y(x)$ by solving equation (25) numerically, use can be made of existing analytical solutions of the problem. Indeed, the family of axisymmetrical surfaces with constant average curvature has been described in 1841 by the mathematician Delaunay [24]. Delaunay showed that this family can be generated by the revolution of the family of 2D curves that are the locus of one the foci of an ellipse, parabole, or hyperbole as it rolls without slipping along the revolution axis. These 2D curves are commonly called elliptic, parabolic, or hyperbolic Delaunay's roulettes, respectively and the constant average curvature of the revolution surfaces that are generated by them is positive, zero, or negative, respectively [25, 26]. The Delaunay's roulettes can be expressed analytically in various ways [23, 26]. We have made use the parametric formulations proposed by Ferréol and Mandonnet [26] , the mathematics of which is summarised in the Appendix of the present paper.

Fig.5 aims at illustrating the shape of a few $y(x)$ curves belonging to the family of Delaunay's roulettes and obtained using values for $\psi/2$ and n_c that are likely to be representative of practical sintering systems : $\psi/2 = 0$ (Fig.5a), $\pi/9$ (Fig.5b) or $2\pi/9$ (Fig.5c) ; $n_c = 6.83$ (full curves) or 10.47 (dotted curves) (corresponding, from (8), to $\beta = \pi/4$ or $\pi/5$, respectively). The graphs on the left hand side of Fig. 5 present a few $y(x)$ curves representative of u values ranging from somewhat below the maximum (x_{min} close to 0, i.e. a very small solid/solid contact area) to less than 0.15 (the actual u values for the different curves does not matter for the following discussion). For each of these curves, the graphs at the right hand side present the variation of the in-plane curvature $H/R_{\text{in plane}}$ as a function of x.

For all curves, the $H/R_{\text{in plane}}$ varies quite widely along x. For the curves with small $x_{\min}$, this variation becomes particularly abrupt close to $x_{\min}$. For $\psi/2 = 0$ (Fig.5a), the curvature decreases with increasing x and remains always positive. In contrast, for $\psi/2 = 2\pi/9$ (Fig.5c), the curvature increases with increasing x and can remain negative all the way (in particular when $\psi/2 > \beta$). For the intermediate case $\psi/2 = \pi/9$ (Fig.5b), both of these two behaviours can be observed depending on the values of β and u.

(Figure 5)

When $\psi/2 \neq 0$ (Fig.5b and c), the curves exhibit an inflexion point (curvature crossing zero) when $x_{\min}$ becomes small enough. In such cases, it was found that u reaches a maximum for a certain $x_{\min}$ value and starts to decrease when $x_{\min}$ further decreases. The interface energy F also presents a minimum when $x_{\min}$ varies in the same range. This indicates that, when $\psi/2 \neq 0$, the formation of the first solid/solid necks between contacting particles at the very early stage of sintering occurs via a transition between two distinct thermodynamic states with different energies. This phenomenon will be further analysed in the future.

3.2 Constant $R_{\text{in plane}}$ approximation

It is tempting to compare the value of the interface energy F (5) derived from the exact solution of the problem to the value of F derived by approximating $Y(X)$ by the equation of an arc of circle. This approximation is represented in Fig.6. If $R = rH$ is the radius of the arc of circle, the boundary conditions (13 - 15) imply that the coordinates (x_0, y_0) of the centre of the circle are

$$x_0 = \tan\beta\left(1 - r\cos\frac{\psi}{2}\right) \tag{26}$$

and $y_0 = r\cos\frac{\psi}{2}$. (27)

The function $y(x)$ then writes

$$y(x) = y_0 - \sqrt{r^2 - (x - x_0)^2} \quad (28)$$

and the limits of integration are

$$x_{\min} = x_0 + r\sin\frac{\psi}{2} \quad (29)$$

and $x_{\max} = x_0 + r\sin\beta$. (30)

Relations (20), (22), and (23) then yield the following analytical expressions :

$$u = \frac{6r^3}{\tan^2\beta}\left\{\begin{array}{l}\frac{1}{3}\left(\cos^3\beta - \cos^3\frac{\psi}{2}\right) + \frac{1}{2}\cos\frac{\psi}{2}\left(\sin^2\beta - \sin^2\frac{\psi}{2}\right) - \\ \frac{1}{2}\tan\beta\left(\frac{1}{r} - \cos\frac{\psi}{2}\right)\left(\sin\beta\cos\beta - 2\cos\frac{\psi}{2}\sin\beta + \cos\frac{\psi}{2}\sin\frac{\psi}{2} + \beta - \frac{\psi}{2}\right) + \\ \frac{1}{2}\left(\cos\beta - \cos\frac{\psi}{2}\right)\left(\sin\beta - \tan\beta\cos\frac{\psi}{2}\right)\left[\frac{\tan\beta}{r} + \frac{2}{3}\left(\sin\beta - \tan\beta\cos\frac{\psi}{2}\right)\right]\end{array}\right\}, \quad (31)$$

$$A_{\mathrm{sl}} = n\,n_{\mathrm{c}}H^2 2\pi r^2\left[\left(\beta - \frac{\psi}{2}\right)\tan\beta\left(\frac{1}{r} - \cos\frac{\psi}{2}\right) - \left(\cos\beta - \cos\frac{\psi}{2}\right)\right], \quad (32)$$

and $A_{\mathrm{ss}} = \frac{n}{2}n_{\mathrm{c}}H^2\pi r^2\left[\tan\beta\left(\frac{1}{r} - \cos\frac{\psi}{2}\right) + \sin\frac{\psi}{2}\right]^2$. (33)

These expressions are valid whatever the value of r, positive or negative. They offer the advantage that, if the constant $R_{\text{in plane}}$ approximation is sufficiently accurate, the partial derivatives of F with respect to $V_{\mathrm{p}}^{1/3}$, n_{c}, and u (i.e. the driving forces for sintering) can also be expressed analytically.

(Figure 6)

The r values that provide the same u values as for the cases dealt with in Fig.5 have been computed by numerical solution of equation (31). For each curve $1/r_{\text{in plane}}(x)$ presented on the right hand side of Fig.5, the computed value of $1/r$ is represented by a vertical arrow pointing on the corresponding point on the curve. Notice that some of the curves drawn for the case $\psi/2 = 2\pi/9$ yield negative r values. As a visual illustration of the difference between the exact and approximate approaches, Fig. 7 shows, for the cases $\psi/2 = 0$, $\beta = \pi/4$, and $u = 0.408$ or $u = 0.065$, the comparison of the exact curves $y(x)$ (full lines) with the corresponding arcs of circles approximations (dotted lines). Quite strikingly, the difference is so small that it cannot be seen unless the graph scales are very widely enlarged. For the arc of circle approximation, $x_{\min}$ is slightly lower whereas $x_{\max}$ is (very) slightly larger (these two effects compensate for one another in such a way as to yield the same u value).

(Figure 7)

The relative difference $\Delta F/F$ between the two approaches was computed from relation (5) using (22), (23), (32), and (33) for a large number of plausible combinations of parameters (among which all the cases corresponding to the curves in Fig.5). The difference was most generally below 5×10^{-4}, which we actually consider to be the level of precision of the numerical computation procedure that was used. The largest differences were found for the largest u values, when the (exact) $y(x)$ curves begins at small $x_{\min}$ (as illustrated in Fig.5, the curvature variation becomes then particularly abrupt close to $x_{\min}$. At very small $x_{\min}$, the arc of circle approximation breaks down when the u value for the exact solution is so large that the arc of circle providing the same u would have to start at a negative $x_{\min}$: the difference between the two approaches can then not be computed. An example of this case is the lowest curve for $\beta = \pi/4$, $\psi/2 = 2\pi/9$ in Fig.5c. For the 16 other curves presented in Fig.5, $\Delta F/F$ did

not exceed 0.1 % except in two cases : the lowest curve drawn for $\beta = \pi/5$, $\psi/2 = 2\pi/9$ in Fig.5c ($\Delta F/F$= 0.24%) and 4.3 % for the lowest curve drawn for $\beta = \pi/4$, $\psi/2 = 0$ in Fig.5a ($\Delta F/F$= 4.3%). Hence, it can be concluded that, for all practical purposes, equations (31) to (33) derived using the arc of circle approximation involve no significant lack of precision (a similar conclusion was established by Heady and Cahn [22] for the case of the shape of a liquid meniscus between two solid spheres).

4 Conclusion

The model developed in this work allows the use of continuous variables for expressing the dependence of the solid/liquid and solid/solid interface areas on the dihedral angle $\psi/2$, liquid volume fraction u and particle coordination n_c. Although an exact solution is mathematically accessible (through numerical solution of a differential equation or using the Delaunay's surfaces), the approximation of the profiles by arcs of circle yields analytical expressions which, for most practical purposes, involve no significant loss of precision. An example of application of the model is the prediction of the influence of u and n_c, on the distribution of liquid in gradient materials processed by liquid phase sintering [12].

Appendix : Analytical formulation for the Delaunay's roulettes

Use was made of the parametric equations proposed by Ferréol and Mandonnet [26] of which the mathematics can be summarised as follows (normalising by the cone height H is done everywhere). The shape of a particular elliptic or hyperbolic roulette is determined by the parameter

$$f = \frac{b}{a} \tag{34}$$

where a and b are the half-axes of the ellipse or hyperbole from which the roulette is generated (there is no need to deal with the intermediate case of the parabolic roulette). The x and y values along the curve $y(x)$ are expressed in terms of a common parametric variable denoted t. The boundary points of the curve $y(x)$ at coordinates (x_{min}, 0) and (x_{max}, y_{max}) are thus determined by the two boundary values t_{min} and t_{max}.

Elliptic roulette

The formulations are much simplified by denoting

$$e = \sqrt{1 - f^2}\,. \tag{35}$$

The parametric equations for x and y are then

$$x = \sqrt{\frac{1 - e\cos t}{1 + e\cos t}} \tag{36}$$

and $$y = f\int_0^t \frac{1}{\sqrt{1 - e^2\cos^2 u}\,(1 + e\cos u)}\,du\,. \tag{37}$$

The t variable is related to the first derivative $y'(x)$ (= $\tan\theta$ on Fig.4) as

$$\sin t = -\frac{f}{e}\frac{1}{y'(x)}\,. \tag{38}$$

Hence, t_{min} and t_{max} straightforwardly derive from conditions (14) and (15). However, two possible t_{min} (and t_{max}) values are solutions of (36) and, depending on the value of the shape parameter f, the right pair of t_{min} and t_{max} needs to be chosen in order to have the slope of the curve to evolve monotonously from $\tan\psi/2$ at t_{min} to $\tan\beta$ at t_{max}.

Hyperbolic roulette

Denoting now

$$e = \sqrt{1 + f^2}\,, \tag{39}$$

the parametric equations for x and y are

$$x = \sqrt{\frac{e - \cos t}{e + \cos t}} \tag{40}$$

and $$y = f\int_0^t \frac{\cos u}{\sqrt{e^2 - \cos^2 u}\,(e + \cos u)}\,du\,. \tag{41}$$

The t variable is related to $y'(x)$ as

$$\tan t = -\frac{f}{e}\frac{1}{y'(x)}. \tag{42}$$

Again, using conditions (14) and (15), the right couple of $t_{\min}$ and $t_{\max}$ needs to be chosen in order to have the slope of the curve to evolve monotonously from $\tan\psi/2$ to $\tan\beta$.

Acknowledgments

The author is indebted to C. Colin and D. Pardoen for their contribution in initiating this work.

REFERENCES

1. Price, G.H.S., Smithells, C.J., Williams, S.V., 1938, J. Inst. Metals, **62**, 239
2. Kingery, W.D., 1959, J. Appl. Phys., **30**, 301
3. Yoon, D.N., Huppmann, W.J., 1979, Acta Metall., **27**, 693
4. Lange F.F., 1984, J. Am. Ceram. Soc., **67**, 83
5. Kaysser, W.A., Zivkovic, M., Petzow, G., 1985, J. Mater. Sci., **20**, 578

6. Mortensen, A., 1997, Acta Materialia, **45**, 749
7. Lisovsky, A.F., 1990, Intern. J. Heat Mass Transfer, **33**, 1599
8. Colin, C., Durant, L., Favrot, N., Besson, J., Barbier, G., Delannay, F., 1993-1994, Int. J. of Refractory Met. & Hard Mater., **12**, 145
9. Mortensen, A., Suresh, S., 1995, Intern. Mater. Rev., **40**, 239
10. Colin, C., Favrot, N., Barbier, G., Delannay, F., 1996, *Proceedings Colloque 'Les traitements des poudres et leurs conséquences* (Paris, Société Française de Métallurgie), 30-1
11. Pardoen, D., Colin, C., Delannay, F., 1998, *Proceedings Colloque National de Métallurgie des Poudres* (Paris, Société Française de Métallurgie), 241
12. Delannay, F., Pardoen, D., Colin, C., 2005, Acta Materialia, **53**, 1655
13. Arzt, E., 1982, Acta Metall., **30**, 1883
14. Scott, G.D., 1962, Nature, **194**, 956
15. Mason, G., 1968, Nature, **217**, 733
16. Deryagin, B.V., 1940, Trans. Faraday Soc., **36**, 203
17. Eversole, W.G., Lahr, P.H., 1941, J. Chem. Phys., **9**, 686
18. Norton, F.H., Johnson, A.L., 1944, J. Amer. Ceram. Soc., **27**, 77
19. Clarke, D.R., 1987, J. Am. Ceram. Soc., **70**, 15
20. Beere, W., 1975, Acta Metall., *23*, 131
21. Park, H.-H., Yoon, D.N., 1985, Metall. Trans. A, **16A**, 923
22. Heady, B., Cahn, W., 1970, Metall. Trans. **1**, 185
23. Cannon, R.M., Carter, W.C., 1989, J. Am. Ceram. Soc., **72**, 1550
24. Delaunay, C.-E., 1841, J. Math. Pures et Appl. Sér.1, **6**, 309
25. Eells, J., 1987, Math. Intelligencer, **9**, 53
26. Ferréol, R., Mandonnet, J., 2001, http://www.mathcurve.com/courbes/courbes2d/delaunay/delaunay.shtml

Figure captions

Figure 1 : (a) Aggregate of solid particles immersed in a fluid that completely fills the pores between the particles ; (b) definition of dihedral angle ψ.

Figure 2 : Shape of a particle embedded inside its associated Voronoï cell. The solid/solid interfaces are represented as located at the position of the cell faces.

Figure 3 : Revolution cone of height H and half angle β at the apex. The average Voronoï cell is modelled as equivalent to n_c such revolution cones containing a fraction u of liquid.

Figure 4 : The curve $Y(X)$ is the intersection of the solid/fluid interface with a plane (X, Y) through the cone axis. The surface occupied by the fluid is divided in two parts S_a and S_b.

Figure 5 : Left hand side : $y(x)$ curves belonging to the family of Delaunay's roulettes ; right hand side : corresponding variation of the in-plane curvature $H/R_{\text{in plane}}$ as a function of x. (a) $\psi/2 = 0$; (b) $\psi/2 = \pi/9$; (c) $\psi/2 = 2\pi/9$. The full curves are for $n_c = 6{,}83$ ($\beta = \pi/4$) and the dotted curves for $n_c = 10{,}47$ ($\beta = \pi/5$).

Figure 6 : Approximation of the curve $Y(X)$ by an arc of circle.

Figure 7 : Comparison of the exact solutions (full lines) for the cases $x_{max} = 0.710$ and $x_{max} = 0.900$ with arcs of circle of radius $r = 0.989$ and 0.341 (dotted lines), which correspond to the same u values.

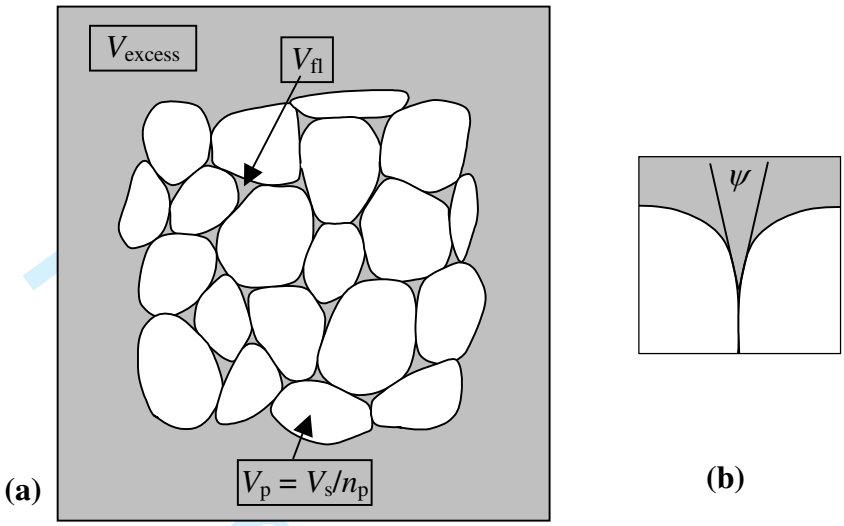

Figure 1 : (a) Aggregate of solid particles immersed in a fluid that completely fills the pores between the particles ; (b) definition of dihedral angle ψ.

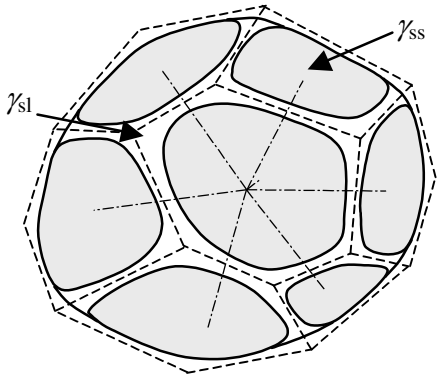

Figure 2 : Shape of a particle embedded inside its associated Voronoï cell. The solid/solid interfaces are represented as located at the position of the cell faces.

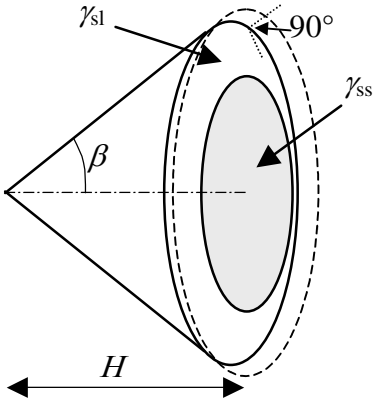

Figure 3 : Revolution cone of height H and half angle β at the apex. The average Voronoï cell is modelled as equivalent to n_c such revolution cones containing a fraction u of liquid.

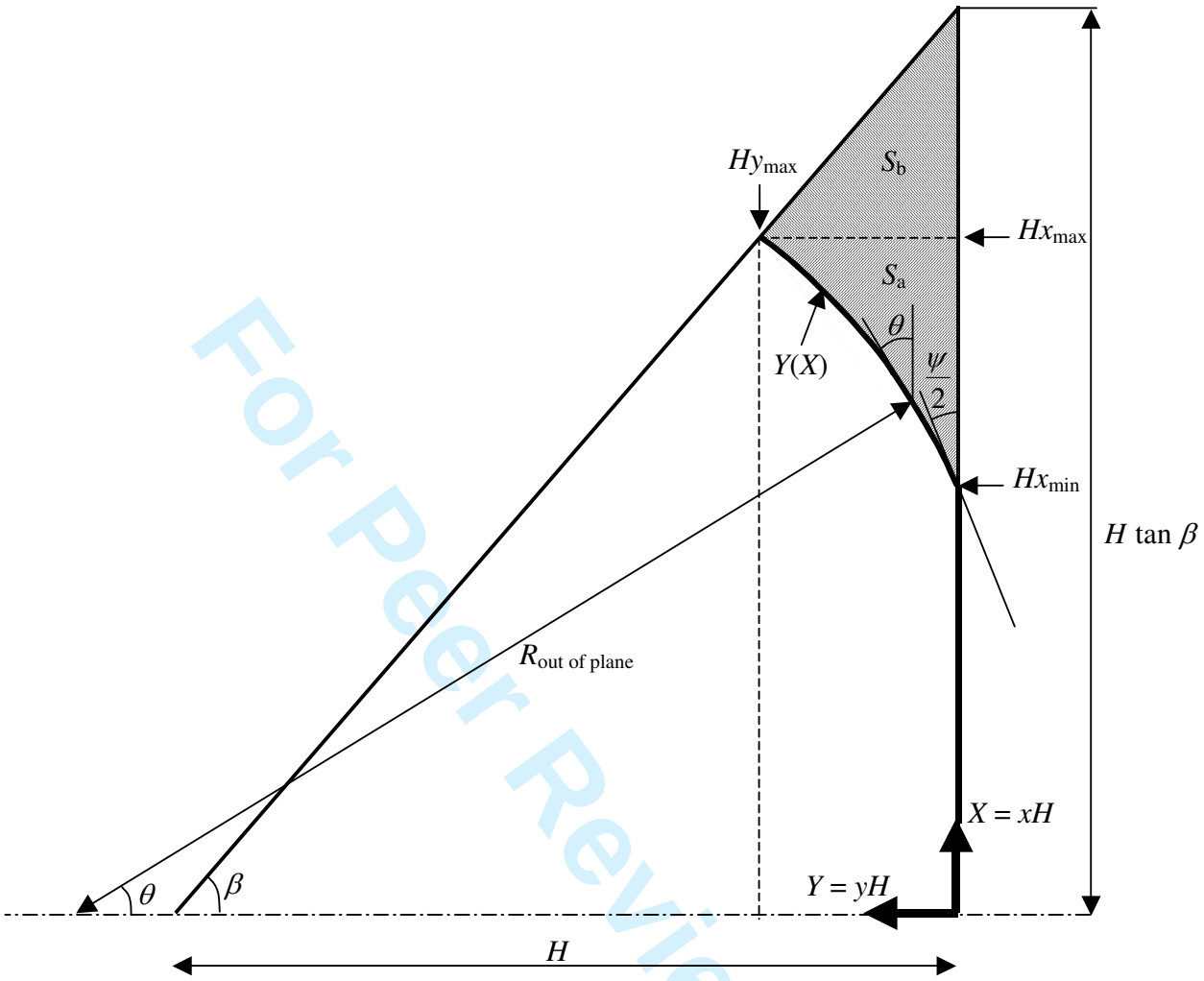

Figure 4 : The curve $Y(X)$ is the intersection of the solid/fluid interface with a plane (X, Y) through the cone axis. The surface occupied by the fluid is divided in two parts S_a and S_b.

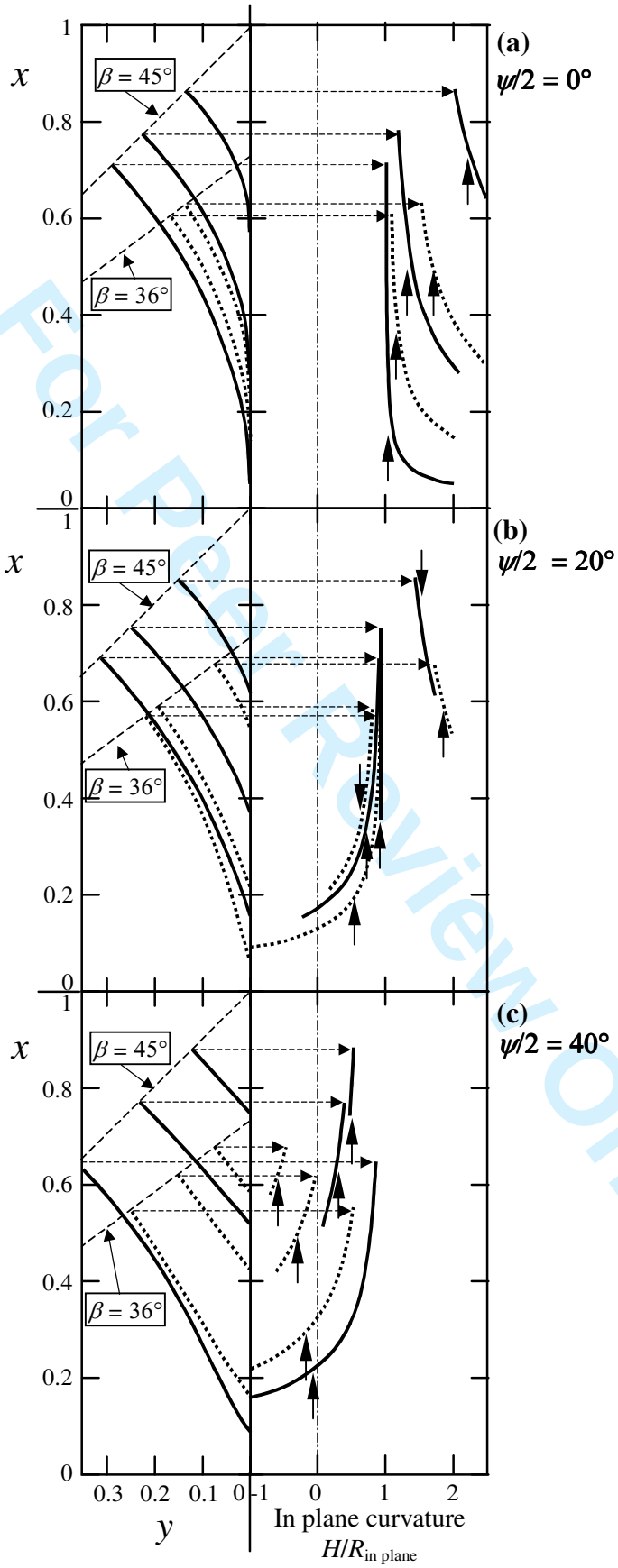

Figure 5

Figure 5 : Left hand side : $y(x)$ curves belonging to the family of Delaunay's roulettes ; right hand side : corresponding variation of the in-plane curvature $H/R_{\text{in plane}}$ as a function of x. (a) $\psi/2 = 0$; (b) $\psi/2 = \pi/9$; (c) $\psi/2 = 2\pi/9$. The full curves are for $n_c = 6{,}83$ ($\beta = \pi/4$) and the dotted curves for $n_c = 10{,}47$ ($\beta = \pi/5$).

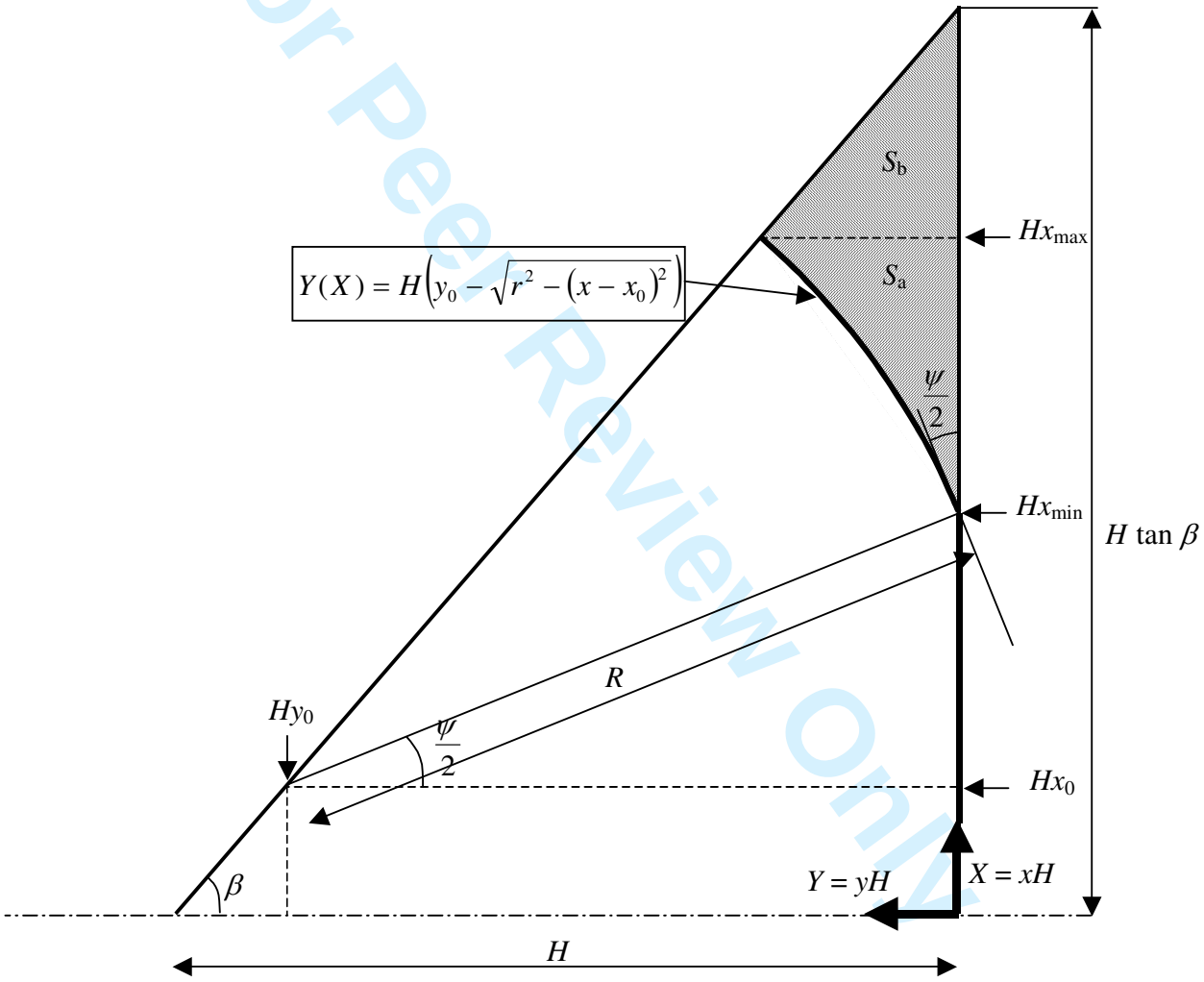

Figure 6 : Approximation of the curve $Y(X)$ by an arc of circle.

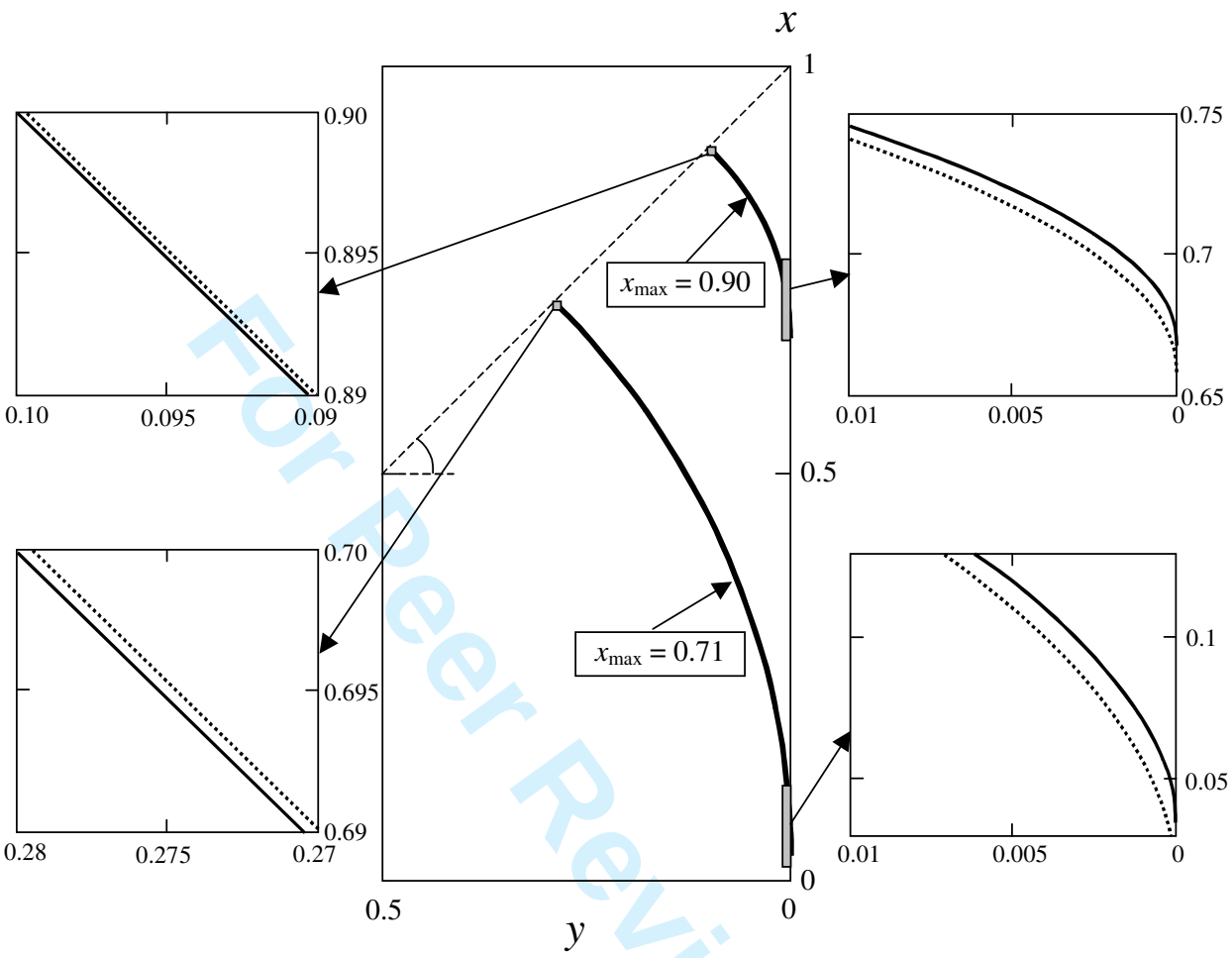

Figure 7 : Comparison of the exact solutions (full lines) for the cases x_{max} = 0.710 and x_{max} = 0.900 with arcs of circle of radius r = 0.989 and 0.341 (dotted lines), which correspond to the same u values.